IL NUOVO CIMENTO Vol. 34 C, N. 6 Novembre-Dicembre 2011
DOI 10.1393/ncc/i2011-11028-3

Colloquia: IFAE 2011

Status of AMS-02 experiment on the International Space Station

S. Di Falco

INFN, Sezione di Pisa - Largo B. Pontecorvo 3, 56100 Pisa, Italy

(ricevuto il 29 Luglio 2011; pubblicato online il 26 Ottobre 2011)

Summary. — The AMS-02 experiment has been installed on the International Space Station on May 19, 2011. The main goals of the experiment are the search for antimatter and dark matter and an high-precision measurement of the spectra of the cosmic rays in the GeV to TeV energy range. This article describes the different components of the detector and presents the performances obtained at the last test beams.

PACS 07.87.+v – Spaceborne and space research instruments, apparatus, and components (satellites, space vehicles, etc.).
PACS 29.40.Vj – Calorimeters.

1. – Introduction

Recent results from space-borne experiments excited a new interest in astroparticle physics, making the search for the missing constituents of the universe (antimatter, dark matter, dark energy,...) one of the most promising fields of discovery for the next years.

In particular the Pamela experiment [1] has measured a $e^+/(e^+ + e^-)$ fraction that shows a large deviation from the predictions of the positron fluxes based on standard models of comsic-ray propagation and interaction: the origin of this discrepancy is still unclear and more precise measurements from AMS are eagerly awaited.

AMS is an international collaboration that includes more than 60 institutes from 16 different countries for a total of more than 500 physicist. The AMS-02 experiment has finally been installed on the International Space Station (ISS) on May 19, 2011 where it will take cosmic data until the end of the ISS life, currently estimated for not earlier than 2020 and, most likely, around 2028. The ISS is orbiting at an altitude of about 386 Km over the earth surface, with a revolution period of 92 minutes and a precession period of 71 days. The maximum of the geographical magnitude is 51.6°. The AMS axis is tilted by 12 degrees with respect to the axis of the ISS.

The numbers of the AMS-02 detector (fig. 1) are quite unusual for a space-borne detector: a volume of $12\,\mathrm{m}^3$ for 7 tons of weight, 20000 electronic channels for a total power consumption of $\sim 2\,\mathrm{kW}$.

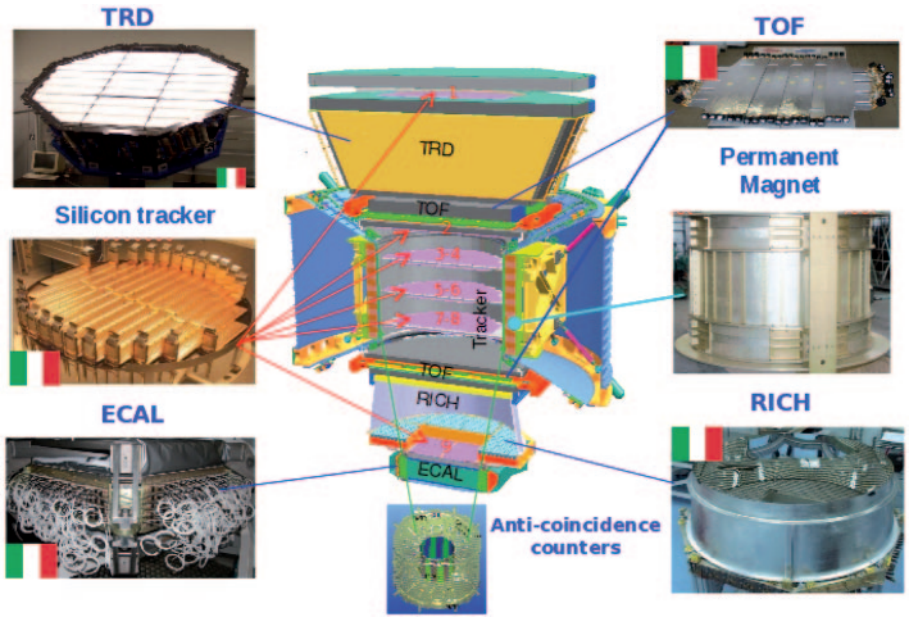

Fig. 1. – The AMS-02 detector: the Italian flags tag subdetectors with Italian contributions.

The different AMS subdetectors are described in the following sections together with their main features and performances measured at the test beams.

2. – The Transition Radiation Detector (TRD): electron/hadron separation

Situated on top of AMS, it's made out of 20 layers of foam and straw tubes filled with a Xe/CO_2 gas mixture [2]. The orientation of the straw tube depends on the layer and allows a 3D tracking. The gas leakage is kept low enough to guarantee the efficiencies of the straw tubes for at least 24 years. Looking at the transition radiation it is possible to distinguish light particles from heavy particles. Test beam results show a rejection factor for protons with respect to positrons better than 10^2 up to 300 GeV, in agreement with Monte Carlo calculations (fig. 2).

3. – The Time of Flight (TOF): time, trigger and charge

The measurement of the time of flight of the particles is performed by 2 stations of scintillators located above and below the Silicon Tracker. Each station is made of 2 layers of scintillator paddles read at both ends by two or three photomultipliers (PMTs). The resolution in time is $\Delta t \simeq 160$ ps, which corresponds to a precision in the speed measurement $\Delta\beta/\beta \sim 4\%$ at $\beta \sim 1$ [3]. The $\mathrm{d}E/\mathrm{d}x$ measurements allow to distinguish the charge of the lightest nuclei. TOF is the main ingredient of the different *charged trigger* streams: *protons* (and antiprotons) together with Anticoincidence Counters, *electrons* (and positrons) together with the Electromagnetic Calorimeter and heavy or slow *nuclei*. Last but not least, TOF is used to distinguish between upgoing and downgoing particles.

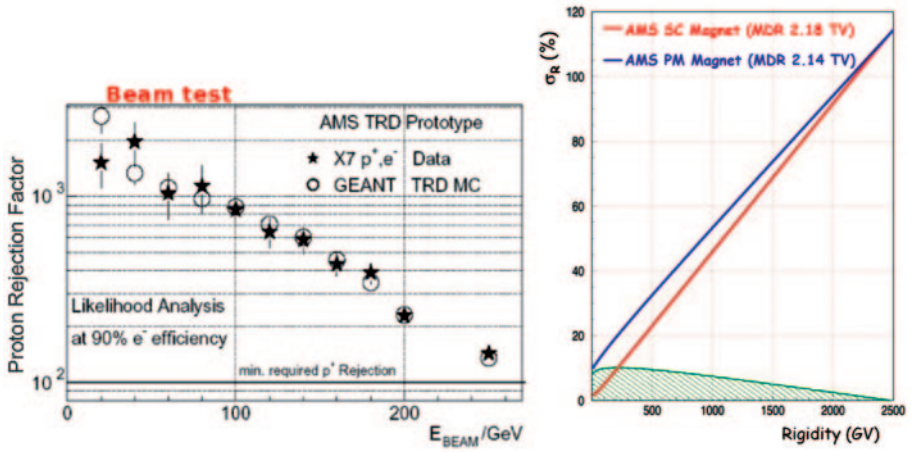

Fig. 2. – Left: TRD rejection factor for protons/positrons as function of energy: comparison between test beam results and Monte Carlo simulation. Right: rigidity resolution and maximum detectable rigidity obtained by the silicon tracker on protons with the current Permanent Magnet layout (upper curve) and the original Superconducting Magnet layout (lower curve): the shaded area shows the difference between the two curves.

4. – The Permanent Magnet (PM)

In the original design of the detector, when AMS was supposed to run only for three years, a very powerful Superconducting Magnet had been chosen. The lifetime of this magnet was limited by the evaporation of the superfluid helium, needed to keep the magnet cold, to not more than 2–3 years.

When the time schedule for the ISS changed, extending AMS running time up to more than 15 years, a permanent magnet became the best choice. The mechanical design of the detector was, by purpose, compatible with the old permanent magnet used for the AMS-01 prototype([1]): a set of permanent dipoles that gives a dipolar magnetic field of 1.5 kG well contained inside the volume of the magnet. After 12 years the intensity of the field of this magnet has been measured to be the same as before, within the 1% accurancy of the measurement.

5. – The Silicon Tracker (ST): momentum, charge and antimatter

The AMS tracker is made of 192 ladders containing the 100 μm pitch silicon strips that measure the two coordinates orthogonal to the detector axis with a resolution of $\sim 10\,\mu$m. The total active area of 6.45 m^2 is disposed on 3 double-sided planes located in the center of the detector (inner tracker) and 3 single-sided planes, respectively located on top of TRD, on top of the PM and between the Ring Imaging Cherenkov and the Electromagnetic Calorimeter (fig. 1); this layer layout allowed to mantain the excellent Maximum Detectable Rigidity (MDR) of the original Superconducting Magnet (fig. 2): 2.1 TV for protons and 3.7 TV for helium nuclei [4]. Momenta lower than $\sim$ 150 GV can be measured using the inner tracker only: in this configuration the acceptance is

([1]) AMS-01 has successfully flown on the Space Shuttle Discovery for 10 days in June 1998.

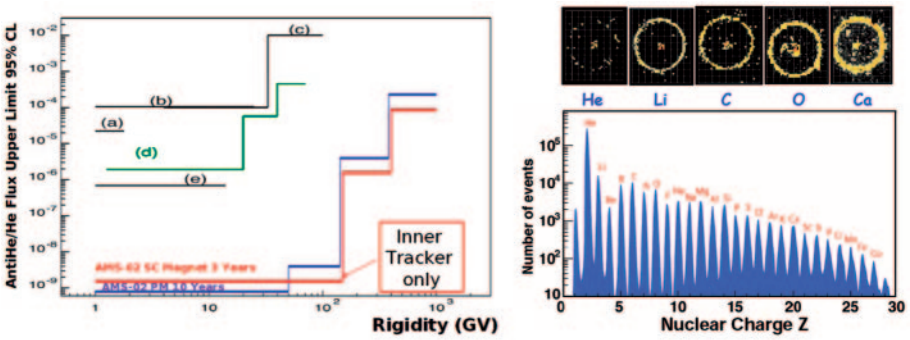

Fig. 3. – Left: limit on anti-helium abundance with respect to helium after 10 years of data taking with the PM; the steps are due to the different acceptance corresponding to the silicon tracker layers used in the momentum fit. Right: charge separation with RICH observing the number of photons produced by a 158 GeV/n ion test beam.

~ 0.5 sr·m^2 and the limit on the abundance of anti-helium relative to helium can be pushed below 10^{-9} in 10 years (fig. 3).

The amplitude of the charge deposited in the silicon sensors allows to measure the charge of the nuclei up to the nickel.

6. – The Anticoincindence Counters (ACC): trigger veto

The Anticoincidence Counters, made of 16 curved scintillators surrounding the silicon tracker, are used in the proton and ion trigger to reject particles entering from the sides of the detector [5].

7. – The Ring Imaging Cerenkov (RICH): speed and charge

This detector consists of a radiator, a reflecting mirror and an array of 10880 photomultiplier anodes [6]. It is able to measure the speed of the particles through their Cerenkov angle with a resolution $\Delta\beta/\beta \sim 0.1\%$. In order to minimize the material in front of the Electromagnetic Calorimeter the radiator is made by 2 different materials with different refraction index and Cherenkov threshold: a silica aerogel at the center ($n = 1.05$, $\beta_{min} = 0.953$) and sodium fluoride ($n = 1.33$, $\beta_{min} = 0.75$) on the sides. By counting the number of the emitted photons it is possible to determine the charge of the nuclei up to nickel (fig. 3) in a redundant way with respect to the ST.

8. – Electromagnetic Calorimeter (ECAL): energy, trigger and dark matter

The last AMS subdetector is a sampling calorimeter made of lead, scintillating fibers and optical glue. It has an active area of $648 \times 648\,\text{mm}^2$, a thickness of 16.7 cm, corresponding to 17 radiation lengths, and a granularity of $9 \times 9\,\text{mm}^2$. Each 10 layer of fibers (a "superlayer") the direction of the fibers is rotated by 90 degrees allowing a 3D reconstruction of the electromagnetic showers. Fibers are read out only at one end by 324 photomultipliers, each divided in 4 anodes. Anodes are read out with a double amplification allowing to span from the MIP energy range (8 MeV) to the TeV particles energy

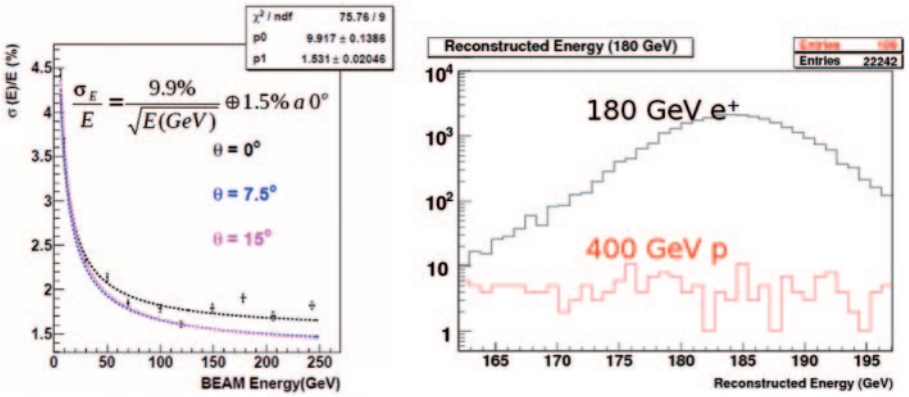

Fig. 4. – Left: energy resolution of the electromagnetic calorimeter. Right: residual 400 proton background in a 180 GeV e^+ after TRD, ECAL imaging and E/P matching selection.

range (up to ~ 60 GeV in one cell). The PMT signal is also used to build an electromagnetic particle trigger that improves the charged particle trigger efficiency on electrons and positrons and gives a $\sim 100\%$ trigger efficiency on photons above 2 GeV [7]. The energy resolution is shown in fig. 4. The energy linearity has been measured to be better than 1% up to 250 GeV while the angular resolution is better than 1° above 50 GeV [8]. The excellent 3D imaging of the electromagnetic shower, together with the TRD identification and the energy/momentum (E/P) matching brings to an electron/hadron rejection factor $> 10^6$: fig. 4 shows the residual background on 180 GeV positrons due to 400 GeV protons normalized with the proper flux as obtained in the August 2010 test beam. The low proton contamination allows a precise determinataion of the positron fraction that could reveal the first signal of dark matter annihilation in e^+e^- (see for example [9]). Other indirect channels involving antiproton or deuterium will also be accessible to AMS.

9. – Conclusion and outlook

Since last May 19 AMS-02 is taking data on the ISS: the detector is performing well, in agreement with the results of the last test beams. The first results should be published quite soon.

REFERENCES

[1] Picozza P. *et al.*, *Nucl. Instrum. Methods Phys. Res. A*, **623** (2010) 672.
[2] Hauler F. *et al.*, *IEEE Trans. Nucl. Sci.*, **51** (2004) 1365.
[3] Amati L. *et al.*, *IEEE Nucl. Sci. Symp. Conf. Rec. 2004*, p. 366.
[4] Haino S., *Nucl. Instrum. Methods Phys. Res. A*, **630** (2011) 78.
[5] Bruch T. and Wallraff W., *Nucl. Instrum. Methods A*, **572** (2007) 505.
[6] Arruda L., Barao F., Goncalves P. and Pereia R., *Nucl. Phys. Proc. Suppl.*, **172** (2007) 32.
[7] Cadoux F. *et al.*, *IEEE Trans. Nucl. Sci.*, **55** (2008) 817.
[8] Di Falco S., *Adv. Space Res.*, **45** (2010) 112.
[9] Kounine A., *ISVHECRI Proceedings*, Batavia (2010).